GEOPHYSICAL RESEARCH LETTERS, VOL. 22, NO. 5, PAGES 575-578, MARCH 1, 1995

# Ice Flow Dynamics of the Greenland Ice Sheet from SAR Interferometry

E. Rignot

Jet Propulsion Laboratory, California Institute of Technology, Pasadena, CA 91109

K.C. Jezek and H.G. Sohn

Byrd Polar Research Center, The Ohio State University, Columbus, OH 43210

**Abstract.** Synthetic-aperture radar (SAR) interferograms produced from ESA's ERS-1 satellite, provide the first synoptic view of ice flow dynamics of the western sector of the Greenland Ice Sheet. Glacial motion is detected in the radar ranging direction at millimetric scales, across a complete sequence of snow accumulation and melting regimes, despite significant variations in their radar scattering properties. Ice flow evolves from a slow, regular motion at the higher elevations. At lower elevations, motion is strongly convoluted by meter-scale undulations in surface topography, which have a unique interferometric signature that enables a novel approach for retrieving flow direction. Inferred flow directions, combined with surface displacements in the radar ranging direction, yield ice velocity estimates that are within 6 % of in-situ measurements gathered along a 40 km survey line. Application of repeat-pass SAR interferometry to the entire Greenland Ice Sheet should enable precise mapping of its ice flow dynamics at an unprecedented level of spatial detail.

## Introduction

Earth's great ice sheets are changing [*Bentley,* 1993; *Van der Veen,* 1991], and these changes can be relatively rapid. The western extent of the Greenland Ice Sheet has measurably varied on generational time scales [*Weidick,* 1991] possibly associated with varying rates of surface melt along its western flank [*Braithwaite,* 1993]. The interior of Greenland is also changing. Variability in precipitation and accumulation patterns [*Bromwich et al.,* 1993; *Steffen et al.,* 1993] may be causing a regional ice sheet thickening, at a rate of 2-10 cm per year based on surface observations [*Van der Veen,* 1993; *Kostecka and Whillans,* 1988; *Reeh and Gundestrup,* 1985], or as much as 10-20 cm per year based on analysis of satellite data [*Zwally et al.,* 1989].



**Paper number 94GL03381**
**0094-8534/95/94GL-03381$03.00**

Changes in ice sheet dynamics are manifest through changes in ice sheet shape and motion. Satellite radar interferometry is one technique that shows promise for measuring very small variations in both parameters [*Zebker et al.,* 1994; *Goldstein et al.,* 1993]. Here, we report on the first SAR interferometry results obtained over the western flank of the Greenland Ice Sheet. Interferograms are presented along a swath that extends from the Jacobshavn Glacier through the ablation and soaked snow facies, to the percolation facies, and to the dry snow facies [*Benson,* 1962] (Fig. 1). The white, snow-covered surface is nearly featureless in optical and SAR-intensity imagery, but highly detailed information on ice motion is revealed in the SAR interferograms.

## Observations

To obtain an ERS-1 SAR interferogram, two images acquired a few days apart along the same orbit of the spacecraft, are registered with sub-pixel accuracy, and the phase values of the radar signals are differenced, condensed and averaged together. The measured phase shifts, $\delta\phi$, are conditioned by the radar wavelength $\lambda$ (5.6 cm), the baseline separation, $B$, between the two slightly different positions of ERS-1 when the radar data for the two images were obtained, the surface topography, $H$, and the surface motion vector, $\mathbf{V}$, as

$$\delta\phi = \frac{4\pi}{\lambda} \left[ B\ cos(\alpha + \theta(H)) + \delta t \mathbf{V} \cdot \mathbf{r} \right]. \qquad (1)$$

$\alpha$ is the baseline angle with respect to horizontal, $\mathbf{r}$ is the unit range vector from the radar antenna to a point on the ground, $\delta t$ is the time separation in between the two passes (3 days), and $\theta(H)$ is the topography-dependent angle of $\mathbf{r}$ with respect to horizontal. We estimated $B$ from ESA's precision orbits. Because $B$ was short (26 m) and the ice sheet is gently undulating at that location, the phase shift introduced by surface topography was only of the order of a fraction of a fringe ($2\pi$ variation in $\delta\phi$) across the ERS-1 SAR swath. This phase shift was calculated and removed from $\delta\phi$ by registering the data to a digital elevation model of Greenland produced from radar altimetry data, at 2 km sample spacing, with 10-20 m vertical accuracy [*Ekholm*

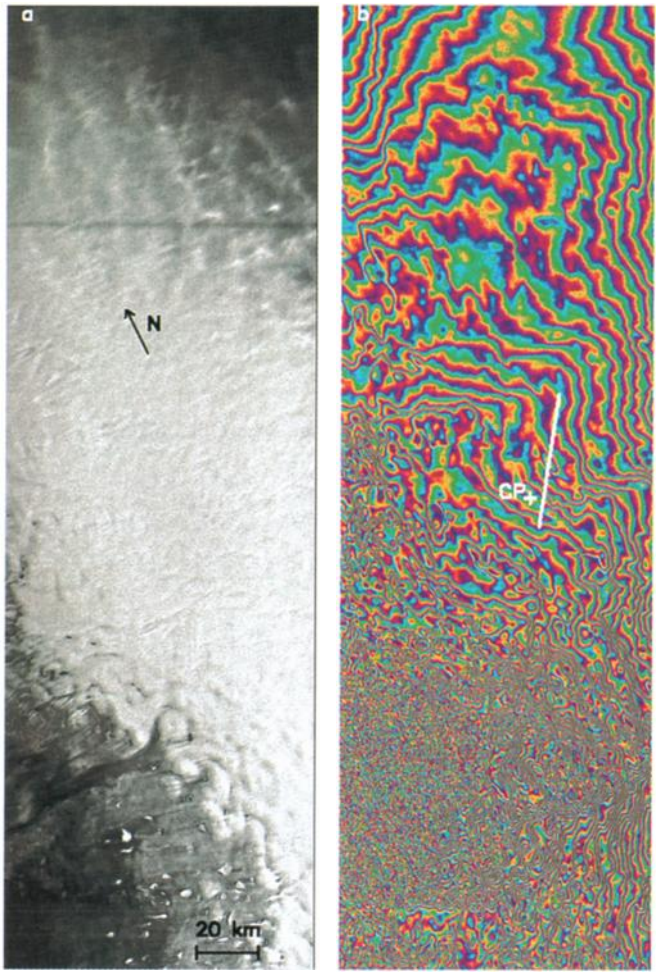


**Figure 1.** (a) ERS-1 SAR mosaic, 300 km x 100 km in size, acquired on 11-28-91 over the western flank of the Greenland Ice Sheet © ESA 1991. ERS-1 flies from top to bottom, looking to its right. The radar-bright percolation facies separate the radar-dark ablation (very dark) and soaked-snow (dark) facies to the south from the dry-snow (very dark) facies to the north; (b) Interferogram obtained with a pair of ERS-1 SAR images acquired on 11-25-91 and 11-28-91 and indicative of ice motion. Going from blue through yellow and red to blue again corresponds to a 28 mm movement toward the radar.

*et al.*, 1994]. The phase values were then unwrapped [*Goldstein et al.*, 1988], referenced to a point of known surface velocity, and converted into absolute surface displacements. A second reference surface velocity was used to correct for small along-track variations in $B$ (< 2 m), as such changes affect the fringes in a manner similar to a velocity gradient. Even with these two references, the interferogram is controlled by at least four processes: 1) flow speed, 2) flow direction; 3) surface slope; and 4) the radar scattering properties of the firn.

In the percolation facies, a network of wavelength-sized, buried (50 cm of dry snow in November), ice bodies, formed as a consequence of summer melt, provides the dominant source of scattering [*Rignot et al.*, 1993; *Jezek et al.*, 1994]. Their radar echoes are one order of magnitude brighter than that recorded for the firn volume or the snowy surface. In the soaked snow facies, more vigorous summer melt leaves a superimposed ice zone which is too homogeneous to yield strong backscatter. In the dry snow facies, volume scattering from the firn dominates, but also yields weak radar echoes. Hence, across the different snow and accumulation regimes, the intensity images and the fringe patterns are more related to the volume properties of the firn than to the ice sheet surface.

With that background, a general picture of ice sheet flow can be established by examination of Fig. 1b. A camp was established near the center of the scene in 1991 to obtain detailed physical property measurements along a 40 km survey line. North and east of the camp, the fringes are parallel and trend roughly north-south (Fig. 2). West of the camp, the fringes re-orient and the fringe rate decreases. Yet, we cannot unambiguously interpret this pattern as either a change in flow direction or a change in flow speed since we are limited to a single projected view of the motion field.

Farther to the south and west of the survey line, the fringe patterns become more complicated. Here, the flow direction may be determinable because of concentrations of concentric pairs of fringes. These pairs arise from motion, mostly vertical, over shallow, meter-scale bumps or depressions. The effect is illustrated in Fig. 3 where a modeled interferogram is compared to a real interferogram extracted from Fig. 1b. The model demonstrates that the line connecting the concentric circles is in the flow direction. Moreover, the distance between the centers of the concentric circles is approximately half the width of the bump, and the phase difference measured between the center of a circle and the local mean phase is related to the height of the bump. From the model, we estimate that most bumps and hollows in Fig. 2 are a few km's across and a few 10's of m in height. This new technique allows for an independent estimation of flow direction using a single projected view of the ice motion field. The inferred flow directions are consistent with the flow vectors derived from conventional surveying (Fig. 2). They also help interpret the fringe pattern west of the camp as primarily caused by a 15° change in flow direction.

Along the survey line, we converted the surface displacements into ice velocities using the flow direction indicated by pairs of concentric circles both north and south of the survey line and linearly interpolated in between. We assume a surface flow parallel to the ice sheet surface. Surface slope is computed from the digital elevation model. The results are within 6 % on average of the in-situ measurements (Fig. 4). The difference between the two estimates reaches 15 % in the southern section of the survey line. Surface slopes would have to be in error by more than 2° to explain those differences, but surface slopes usually do not exceed 1°. Flow directions would have to be in error by up to 10°, but in-situ

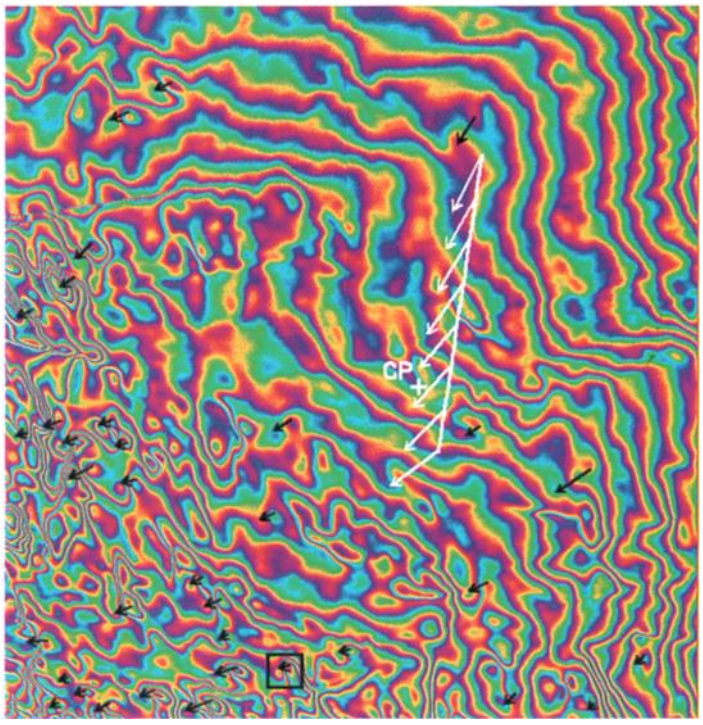


**Figure 2.** Details of the central part of Fig. 1b. A camp was established at 69.87° north, 47.11° west (vertical cross mark) in 1991 to measure topography, ice velocity and snow accumulation rate. The survey line and 8 velocity vectors are shown in white. A limited number of vectors connecting pairs of concentric fringes are shown in black. The orientation of the vectors is indicative of flow direction. Their length is equal to the distance between concentric circles - not to ice velocity.

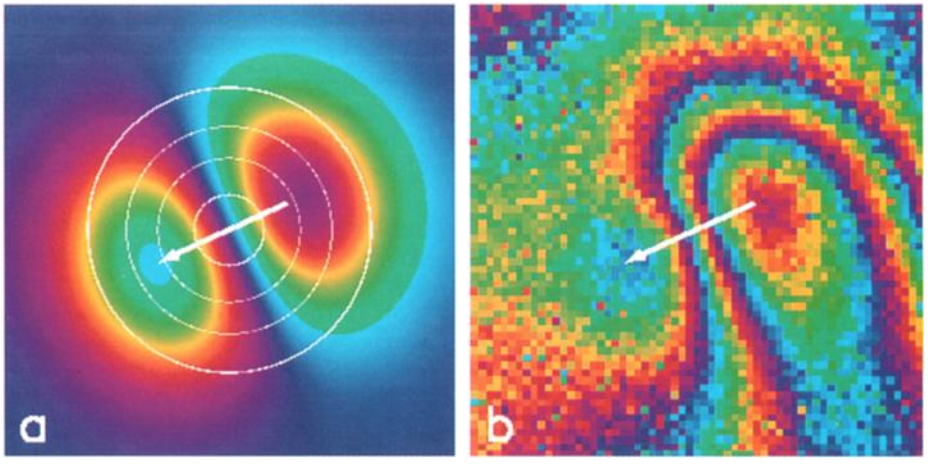


**Figure 3.** (a) Interferogram simulating ice flow over a bump. Contour lignes (20 m) are shown as white lines. The flow velocity is 30 cm/day, 25° counterclockwise from top. The bump is of Gaussian shape and the ice flow is assumed parallel to the surface. (b) Fringe patterns within the 4.8 km open white square in Fig. 2. Differences between (a) and (b) probably are caused by the non-gaussian shape of the real bump.

estimates are known within ±2° and flow directions inferred from the fringe patterns within ±4°. Changes in snow thickness of about 10 cm between the two passes could however account for the difference [*Jezek and Rignot*, unpublished manuscript, 1994]. Hence, we believe a combination of errors in flow directions and changes in snow thickness may explain the discrepancy.

Fringes in the northerly portion of the swath (Fig. 1b) are slowly changing. In contrast, the southerly portion becomes increasingly complicated as the dynamics associated with the vigorous flow of the Jacobshavn Glacier begin to dominate. Within the main body of ice stream flow (the long dark stretch visible in the bottom left of Fig. 1a), the flow direction is almost perpendicular to that at the survey line, with strong velocity gradients, and flow speeds up to 140 cm/day (H. Brecher, personal communication). The resulting phase variations are so rapid that we are unable to resolve the fringes because of pixel size limitations. There, a revisit time of one day is required to map ice velocity.

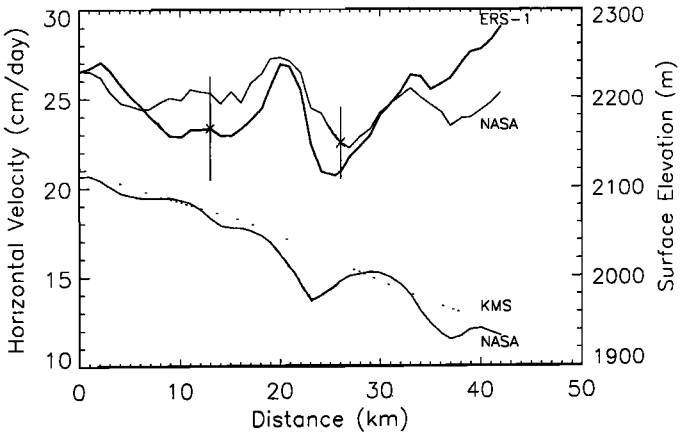


**Figure 4.** Comparison of the SAR-derived velocities (labeled ERS-1) with 43 in-situ measurements (labeled NASA) gathered along the survey line, starting from North. The ±2 cm/day error bar for the in-situ measurements results from absolute location errors in the position of the stakes deployed on the ice sheet to measure horizontal displacements over a 300-day period between 1991 and 1992. The error bar for the ERS-1 velocities results from a $\pm 4^{o}$ uncertainty in flow direction. The surface elevation measured in-situ (labeled NASA), and the radar altimetry data (labeled KMS) are shown in continuous and dotted lines.

## Conclusions

Interference fringes can be constructed across regions of dramatically different snow properties. It is also possible to estimate ice flow direction and ice velocity with a single interferometric observation in areas that contain km scale bumps and hollows, several 10's of m in height. In other areas, surface measurements of at least two velocity vectors several tens of kilometers apart, are essential to bound the interpretation of the SAR interferometry. Once the validation is in hand, the detail on ice velocities derivable from spaceborne SAR interferometry is unprecedented by any other technique.

**Acknowledgments.** This worked was funded by grants from NASA's Polar Oceans and Ice Sheets Program. We thank Simon Ekholm for providing the elevation model of Greenland; Robert H. Thomas and Karl Kuivinen for providing information from their in-situ measurements; Gilles Peltzer for discussions on the fringe patterns; and Jakob van Zyl for comments on the manuscript.

## References

Benson, C., Stratigraphic Studies of the Snow and Firn of the Greenland Ice Sheet, *US Army Snow Ice and Permafrost Res. Estab. Res. Rep. 70*, 1962.

Bentley, C.R., Antarctic Mass Balance and Sea Level Change, *EOS, 74*, 50, 585-586, 1993.

Braithwaite, R.J., Is the Greenland Ice Sheet Getting Thicker?, *Climate Change, 23*, 379-381, 1993.

Bromwich, D.H., F.M. Robasky, R.A. Keen, and J.F. Bolzan, Modeled Variations of Precipitation over the Greenland Ice Sheet, *J. of Climate, 6*, 1253-1268, 1993.

Ekholm, S., R. Forsberg and J. Brozena, Accuracy of Satellite Altimeter Elevations over the Greenland Ice Sheet, *J. Geophys. Res.*, In Press, 1994.

Goldstein, R.M., H. Engelhardt, B. Kamb and R. Frolich, Satellite Radar Interferometry for Monitoring Ice Sheet Motion: Application to an Antarctic Ice Stream, *Science, 262*, 1525-1530, 1993.

Goldstein, R.M., H.A. Zebker and C.L. Werner, Satellite Radar Interferometry: Two-dimensional Phase Unwrapping, *Radio Science, 23*, 713-720, 1988.

Jezek, K.C., S.P. Gogineni and M. Shanbleh, Radar Measurements of Melt Zones on the Greenland Ice Sheet, *Geophys. Res. Lett., 21*, 33-36, 1994.

Kostecka, J.M. and I.M. Whillans, Mass Balance Along Two transects of the west side of the Greenland Ice Sheet, *J. Glaciol., 34*, 31-39, 1988.

Reeh, N. and N.S. Gundestrup, Mass Balance of the Greenland Ice Sheet at Dye-3, *J. Glaciol., 31*, 198-200, 1985.

Rignot, E., S. Ostro, J.J. van Zyl and K.C. Jezek, Unusual Radar Echoes from the Greenland Ice Sheet, *Science, 261*, 1710-1713, 1993.

Steffen, K., W. Abdalati and J. Stroeve, Climate Sensitivity Studies of the Greenland Ice Sheet Using Satellite AVHRR, SMMR, SSMI and In Situ Data, *Meteorol. Atmos. Phys., 51*, 239-258, 1993.

Van der Veen, C.J., State of Balance of the Cryosphere, *Reviews of Geophysics, 29*, 433-455, 1991.

Van der Veen, C.J., Interpretation of Short-Term Ice-Sheet Elevation Changes Inferred from Satellite Altimetry, *Climate Change, 23*, 383-405, 1993.

Weidick, A., Present-day Expansion of the Southern Part of the Inland Ice Sheet, *Rapp. Gronlands Geol. Unders., 152*, 73-79, 1991.

Zebker, H.A., C.L. Werner, P.A. Rosen and S. Hensley, Accuracy of Topographic Maps Derived from ERS-1 Interferometric Radar, *IEEE Trans. Geosc. and Rem. Sens., 32*, 823-836, 1994.

Zwally, H.J., A.C. Breener, J.A. Major, R.A. Bindschadler and J.G. Marsh, Growth of the Greenland Ice Sheet: Measurement, *Science, 246*, 1587-1589, 1989.

E. Rignot, Jet Propulsion Laboratory, MS 300-243, California Institute of Technology, 4800 Oak Grove Drive, Pasadena, CA 91109.

K. C. Jezek and H. G. Sohn, Byrd Polar Research Center, Byrd Polar Research Center, The Ohio State University, Columbus, OH 43210.

(received September 10, 1994;
accepted October 31, 1994.)